Macroscale description of electrokinetic flows at large zeta potentials: Nonlinear surface conduction

Ory Schnitzer and Ehud Yariv
Department of Mathematics, Technion-Israel Institute of Technology, Technion City, Haifa 32000, Israel
(Received 30 May 2012; revised manuscript received 26 July 2012; published 15 August 2012)

For highly charged dielectric surfaces, the asymptotic structure underlying electrokinetic phenomena in the thin-double-layer limit reshuffles. The large counterion concentration near the surface, associated with the Boltzmann distribution in the diffuse layer, supports appreciable tangential fluxes appearing as effective surface currents in a macroscale description. Their inevitable nonuniformity gives rise in turn to comparable transverse currents, which, for logarithmically large zeta potentials, modify the electrokinetic transport in the electroneutral bulk. To date, this mechanism has been studied only using a weak-field linearization. We present here a generic thin-double-layer analysis of the electrokinetic transport about highly charged dielectric solids, which is not restricted to weak fields. We identify the counterion concentration amplification with the emergence of an internal boundary layer—within the diffuse part of the double layer—characterized by distinct scaling of ionic concentrations and electric field. In this multiscale description, surface conduction is conveniently localized within the internal layer. Our systematic scheme thus avoids the cumbersome procedure of retaining small asymptotic terms which change their magnitude at large zeta potentials. The electrokinetic transport predicted by the resulting macroscale model is inherently accompanied by bulk concentration polarization, which in turn results in nonlinear bulk transport. A novel fundamental subtlety associated with this intrinsic feature, overlooked in the weak-field approximation, has to do with the ambiguity of the "particle zeta potential" concept: In general, even uniformly charged surfaces are characterized by a nonuniform zeta-potential distribution. This impairs the need for a careful identification of the dimensionless number representing the transition to large zeta potentials.

DOI: 10.1103/PhysRevE.86.021503 PACS number(s): 66.10.Ed, 47.57.−s, 46.15.Ff, 82.70.Dd

I. INTRODUCTION

A. Background

When a solid surface is brought into contact with a liquid electrolyte, an electrical double layer instantaneously develops about the solid-liquid interface, consisting of immobile surface charge on the solid and a diffuse cloud (the "Debye layer") within the liquid wherein counterions are in excess and coions in deficit. For realistic values of salt concentrations in aqueous electrolytes, the Debye thickness $1/\kappa^*$ of the diffuse layer ranges between the nanometer and submicron range, typically much smaller than the length scale a^* characterizing both natural colloidal systems and man-made microfluidic devices.

When the solid-liquid system is brought out of equilibrium, as under the application of an external electric field, the nonlinear governing equations become formidable, hindering both mathematical and numerical solutions. Fortunately, the scale disparity represented by the smallness of $\delta = 1/\kappa^* a^*$ allows for an approximate mathematical analysis using a boundary-layer paradigm, where the fluid domain is decomposed into a thin Debye layer in quasiequilibrium and an electroneutral "bulk" surrounding it. The first analysis of this limit was carried out by Smoluchowski [1], who calculated the velocity of a spherical particle driven by a uniform electric field, predicting an electrophoretic mobility proportional to the particle zeta potential.

Another route which allows for approximate solutions of out-of-equilibrium problems employs a *weak-field* approximation; it is not limited to thin double layers. Thus, Wiersema [2] was able to solve the resulting linearized set of equations for an electrophoresis problem in which δ appears as a parameter. These calculations were significantly improved by O'Brien and White [3], allowing to address considerably larger values of ζ, the particle zeta potential normalized with the thermal voltage. At small δ values, the numerically calculated mobility increases linearly with ζ, in agreement with Smoluchowski's prediction. This agreement, however, breaks down at moderately large ζ, where the numerical solution exhibits a maxima at a zeta-potential value that increases slowly with diminishing δ.

O'Brien and White [3] were apparently unaware of Dukhin's thin-double-layer analysis of weak-field electrophoresis, which has actually predicted a mobility maxima [4]. As observed by Dukhin, the exponential Boltzmann distribution within the narrow diffuse layer gives rise to large counterion concentrations near the solid surface even at moderately-large zeta potentials. The associated counterion fluxes parallel to the surface, normally negligible in the thin-double-layer limit $\delta \to 0$, emerge at the leading-order ionic conservation equation [5]. This "surface conduction" mechanism was originally addressed by Bikerman [6]; among other things, it results in a nonmonotonic variation of the electrophoretic mobility with the particle zeta potential.

Three years after the publication of the seminal O'Brien and White paper, O'Brien and Hunter [7] simplified and corrected the derivation of Dukhin's mobility formula. Later, O'Brien [8] analyzed a generic problem, not restricted to any specific geometry, using the same set of approximations (weak field and thin double layer), thereby obtaining effective boundary conditions. Formally, surface conduction becomes significant in the thin-double-layer limit when the zeta potential is "logarithmically large,"

$$e^{|\zeta|/2} \sim O(\delta^{-1}). \tag{1.1}$$

Thus, the twofold limit of thin double layers and high surface charge is represented by the limit process of $\delta \to 0$ with $\delta e^{|\zeta|/2}$

 ©2012 American Physical Society

fixed, the latter group motivating the definition of appropriate Bikerman (and Dukhin) numbers [6].

While (1.1) formally entails $|\zeta| \to \infty$, it practically implies that even moderately large ζ values may result in appreciable deviations from Smoluchowski's formula. Indeed, the thin-double-layer mobility approximation of O'Brien and Hunter [7] is in excellent agreement with the numerical results of O'Brien and White [3] at small values of δ.

Following the work of O'Brien and coworkers, the role of surface conduction was investigated in various contexts, including electroviscous forces [9,10], Dielectric enhancement [11,12], and diffusophoresis [13]. More recent analyses, motivated by microfluidic applications, include surface conduction effects on electrokinetic flows over patterned surfaces [14] and, following Ref. [15], surface-charge discontinuities [16], as well as the arrest [17] of flow amplification triggered by the combination of hydrodynamic and electrokinetic slip.

B. Beyond the weak-field approximation

All of the above-mentioned bodies of work are based on the weak-field linearized equation set, describing small departures from equilibrium (both within and outside the double layer). This assumption is unrealistic in many practical situations; in the case of electrophoresis of a micron-size particle, for instance, the application of rather moderate electric fields, say, of magnitude $100\,\mathrm{V\,cm^{-1}}$, results in a voltage drop across the particle which is several multiples of the thermal voltage. Clearly, then, the artificial linearized model cannot capture many of the rich nonlinear phenomena observed in electrokinetic transport [18]. It is, therefore, desirable to derive a macroscale model which, unlike that of O'Brien [8], is not restricted to weak fields.

An attempt in that direction was carried out by Chu and Bazant [19]. Their macroscale model is, however, focused on conducting surfaces; while such surfaces may be common in microfluidic applications, they are the exception rather than the rule in colloidal systems. More importantly, the analysis of Chu and Bazant [19] completely ignores the presence of electrokinetic flow, which is an integral part of virtually any nonequilibrium process. Since the appropriate Péclet number is inherently $O(1)$ for moderate fields [see (2.4) *et seq.*], this flow significantly affects electrochemical transport; as a matter of fact, ionic advection by electrokinetic flow may be neglected only for weak fields, which is exactly the limitation Chu and Bazant [19] have attempted to do away with.

Our goal is to derive a generic macroscale model in the thin-double-layer limit, not restricted to weak fields. We begin by formulating the exactly posed electrokinetic problem; in doing so, we do not commit to a specific geometry or problem type and, accordingly, leave open the specific form of any possible far-field conditions or integral constraints. We then exploit the thin-double-layer limit in a twofold procedure, where we first obtain an approximate description in the electroneutral region and then derive effective "boundary conditions" representing asymptotic matching with the Debye layer. This is essentially the paradigm used by O'Brien [8], who, however, started with the linearized version of the exact problem.

With the Debye layer appearing only implicitly, the resulting macroscale model—albeit still nonlinear—is tremendously simpler than the original exact description. This allows for analytic progress beyond the familiar linear regime. Perhaps more importantly, the absence of scale disparity in this model is appealing to numerical analyses, which would not be required to deal with the resolution of two length scales.

C. Moderate- versus high-charge density

In deriving the proposed macroscale model, we take a step backward, considering first the thin-double-layer limit $\delta \to 0$ associated with *moderate* charge density on the solid surface, where surface conduction does not affect leading-order transport, and only then study the comparable limit of *highly* charged surfaces, defined by the limit process $\delta \to 0$ with a fixed Bikerman (or Dukhin) number, the latter properly defined to represent (1.1). The presentation accompanying this progressive approach serves to elucidate the modifications introduced by the transition to the high-charge regime.

As a matter of fact, a systematic derivation of a macroscale model for moderate surface charges is important on its own right, in view of the common misconceptions in the community regarding the proper description of electrokinetic phenomena in the thin-double-layer limit. The *de facto* standard employed in the literature [20] actually represents a degenerate linear form of the true description, valid only in the absence of concentration gradients. This form, consisting of Laplace's equation governing the electric potential and homogeneous Stokes equations governing the fluid flow, has been obviously attractive to both analytic [21–24] and numerical [25] investigations. Notwithstanding its importance, that linear model cannot be used to analyze problems where concentration polarization plays a major role. For example, it is well known [26] that the generation of direct current by reactive electrodes is naturally accompanied by such polarization.

The derivation of the macroscale model for moderate surface charge follows the standard boundary-layer methodology, wherein the fluid domain is decomposed into two asymptotic regions—charged Debye layer and electroneutral bulk. In the thin-double-layer limit we obtain simplified differential equations within the latter region. The electric potential is not harmonic, whereby Coulomb body forces remain in the Stokes equations. These attributes, foreign to the familiar linear model, are associated with a nonuniform concentration, governed by an advection–diffusion equation.

In deriving a comparable model for highly charged surfaces, we seek to retain the systematic approach implicit by the use of separate asymptotic expansions in different regions of space. This is not a trivial task, since the key feature in the high-charge limit is a scale transition of the Debye-layer variables near the surface. In the intuitive approach of O'Brien and Hunter [7] and O'Brien [8], surface conduction is accounted for by retaining formally small terms that change their relative asymptotic order at large zeta potentials. This raises conceptual questions regarding the proper order of the three limit processes implicit in this scheme—weak field, thin double layer, and high surface charge. In deriving a systematic model not limited to weak fields, we are reluctant to employ this procedure.

We surmount the difficulty associated with scale transition near the surface by conceptually decomposing the fluid domain into *three*, rather than two, asymptotic regions. It was

recognized by Hinch *et al*. [12] that the high-charge limit is associated with the emergence of an *internal* boundary layer, within the Debye layer, where the scaling of the pertinent variables differs (see also Ref. [18]). As a matter of fact, the weak-field analysis of O'Brien [8] makes use of the simplified structure of the governing equations near the surface in calculating the electric potential there (see appendix 1 in that paper).

We here make this idea explicit by treating the internal layer as a separate region in our matched asymptotic analysis. The Debye layer is, consequently, rendered an *intermediate* asymptotic region. In this scheme, no scale transition occurs within the newly defined Debye layer. The literal boundary conditions on the solid surface are now applied to the internal-layer variables, rather than the Debye-layer variables, as is the common practice. The derivation of a macroscale model in the high-charge limit therefore requires separate analysis (and concomitant asymptotic matching) in the electroneutral bulk, the Debye layer, and the internal boundary layer. Formally speaking, the approach of O'Brien and coworkers is tantamount to the use of composite asymptotic expansions [27]; our scheme abandons this rather intuitive method in favor of more systematic Poincaré-type expansions.

The differential equations governing the electro-neutral bulk are the same in both the moderate- and high-charge macroscale models. The difference appears in the effective boundary conditions governing the electrochemical variables. Thus, the homogenous Neumann conditions in the moderate-charge case, which reflect zero ionic fluxes emanating from the Debye layer, are modified to account for counterion fluxes in the high-charge limit. This transformation imparts a dramatic consequence, as it implies concentration polarization even in the absence of an externally applied salt-concentration gradient. The slip condition is also modified.

Since the local Boltzmann distributions within the diffuse part of the double layer depend on the "bulk" salt concentration just outside it, concentration gradients in the electro-neutral bulk naturally imply a nonuniform distribution of the zeta potential along the solid surface—even when it is uniformly charged. (As would become evident, such gradients are inevitable in any nonequilibrium transport process at the high-charge limit.) Thus, the commonly used concept of "particle zeta potential" becomes ambiguous at nonequilibrium. (This ambiguity was overlooked in previous analyses, fixated on the linear regime in the weak-field limit.) With the intrinsic vagueness in the particle-zeta-potential concept, care must be exercised when attempting to define a dimensionless group which would properly represent the transition to large zeta potentials on a global level. The Bikerman number defined here for that purpose is more primitive than the familiar Dukhin number, whose definition is oriented to the weak-field regime.

The structure of this paper is as follows. In the next section we formulate the exactly posed generic electrokinetic problem. The thin-double-layer limit is addressed in Sec. III, where we obtain the approximate differential equations governing transport in the electroneutral bulk. The derivation of the effective boundary conditions in the moderate-charge limit is performed in Sec. IV, while its breakup at large zeta potentials is discussed in Sec. V. A comparable derivation of the effective boundary conditions for highly charged surfaces is detailed in Sec. VI. The neglect of nondilute effects is addressed in Sec. VII. The two macroscale models are recapitulated in Sec. VIII; both are illustrated in Sec. IX via the prototypic problem of particle electrophoresis. We discuss our results and suggest future research directions in Sec. X.

Readers who are interested in the final outcome of the paper, namely the macroscale model, can skip directly from Sec. II to Sec. VIII.

II. FORMULATION OF THE GENERIC PROBLEM

We consider a generic electrokinetic problem wherein a dielectric chemically inert solid is in contact with a symmetric electrolyte solution (valencies $\pm\mathcal{Z}$) whose two ionic species are characterized by their diffusivities $D^{*\pm}$ (dimensional quantities being hereafter decorated by an asterisk). This solution is treated as a dielectric Newtonian liquid (permittivity ϵ^*, viscosity μ^*).

A Debye double layer is instantaneously formed at the solid-electrolyte interface. It comprises an immobile layer of surface charge on the solid surface S, whose density is assumed uniform, together with an oppositely charged diffuse layer within the liquid phase, of characteristic width $1/\kappa^*$. In addition to this Debye width, the system is also characterized by a *geometric* scale a^*, usually a typical linear dimension (e.g., radius of curvature) of the solid surface.

When this system is subjected to an external "force" (an imposed electric field, concentration gradients, etc.) it cannot remain in equilibrium. This results in various transport phenomena and, specifically, relative fluid motion between the solid and the electrolyte. We consider the large class of problems where these phenomena appear steady at a reference frame attached to the solid surface.

We employ a dimensionless formulation, normalizing length variable by a^*, ionic concentrations by a reference concentration c^* [see (2.18)], and electric potentials by the thermal scale ($\approx$26 mV for univalent solutions at room temperature),

$$\varphi^* = \frac{k^*T^*}{\mathcal{Z}e^*}, \tag{2.1}$$

in which k^*T^* is the Boltzmann temperature and e^* the elementary charge. Stress variables are normalized by the Maxwell scale $M^* = \epsilon^*\varphi^{*2}/a^{*2}$ and velocity variables by a^*M^*/μ^*.

A. Governing equations

The electrokinetic transport is described in terms of the two ionic concentrations $c^{\pm}$, the electric potential φ, the velocity field $\mathbf{u}$, and the pressure p. Within the fluid, these variables satisfy the following:

(1) Ionic conservation equations,

$$\boldsymbol{\nabla}\cdot\mathbf{j}^{\pm} + \alpha^{\pm}\mathbf{u}\cdot\boldsymbol{\nabla}c^{\pm} = 0. \tag{2.2}$$

Here, the molecular ionic fluxes $\mathbf{j}^{\pm}$ (respectively normalized by $D^{*\pm}c^*/a^*$) are provided by the Nernst-Planck expressions

$$\mathbf{j}^{\pm} = \mp c^{\pm}\boldsymbol{\nabla}\varphi - \boldsymbol{\nabla}c^{\pm} \tag{2.3}$$

describing transport due to the combined action of electromigration and diffusion. The dimensionless groups

$$\alpha^{\pm} = \frac{\epsilon^* \varphi^{*2}}{\mu^* D^{*\pm}}, \tag{2.4}$$

multiplying the advection terms represent the drag coefficients of the two types of ions. These groups are independent of both system dimension a^* and electrolyte concentration c^*; for typical diffusivities ($\approx 10^{-9}$ m^2 s^{-1}) in univalent aqueous solutions ($\mu^* \approx 10^{-3}$ kg m^{-1} s^{-1}) they are ≈ 0.5 [28].

(2) Poisson's equation,

$$-2\delta^2 \nabla^2 \varphi = c^+ - c^-. \tag{2.5}$$

Here

$$\delta = \frac{1}{\kappa^* a^*}. \tag{2.6}$$

is the dimensionless Debye thickness, wherein

$$\kappa^{*2} = \frac{2\mathcal{Z} e^* c^*}{\epsilon^* \varphi^*}. \tag{2.7}$$

(3) The continuity

$$\boldsymbol{\nabla} \cdot \mathbf{u} = 0 \tag{2.8}$$

and inhomogeneous Stokes equations

$$\boldsymbol{\nabla} p = \nabla^2 \mathbf{u} + \nabla^2 \varphi \boldsymbol{\nabla} \varphi, \tag{2.9}$$

governing the motion of the fluid subject to Coulomb body forces. The latter can be alternatively written

$$\boldsymbol{\nabla} \cdot (\mathsf{N} + \mathsf{M}) = \mathbf{0} \tag{2.10}$$

in which N is the Newtonian stress

$$\mathsf{N} = -p\,\mathsf{I} + (\boldsymbol{\nabla}\mathbf{u}) + (\boldsymbol{\nabla}\mathbf{u})^{\dagger} \tag{2.11}$$

(with $\dagger$ denoting dyadic transposition and I denoting the idemfactor) and M the Maxwell stress

$$\mathsf{M} = \boldsymbol{\nabla}\varphi\boldsymbol{\nabla}\varphi - \tfrac{1}{2}\boldsymbol{\nabla}\varphi \cdot \boldsymbol{\nabla}\varphi\,\mathsf{I}. \tag{2.12}$$

The boundary conditions on the stationary solid surface S are specified in terms of the unit normal $\hat{\mathbf{n}}$ pointing into the fluid. They consist of the following:

(1) Impermeability and no-slip conditions,

$$\mathbf{u} = \mathbf{0} \quad \text{on} \quad S. \tag{2.13}$$

(2) No-flux conditions

$$\hat{\mathbf{n}} \cdot \mathbf{j}_{\pm} = 0 \quad \text{on} \quad S, \tag{2.14}$$

representing the inability of the solution ions to discharge on the chemically inert solid surface.

(3) Gauss's boundary condition, relating the electric displacements in both the liquid and solid media to σ, the uniform surface-charge density (normalized by $\epsilon^*\kappa^*\varphi^*$) on S,

$$\frac{\partial \varphi}{\partial n} = -\delta^{-1}\sigma + \gamma \frac{\partial \varphi_s}{\partial n} \quad \text{on} \quad S. \tag{2.15}$$

Here $\partial/\partial n = \hat{\mathbf{n}} \cdot \boldsymbol{\nabla}$, φ_s is the electric potential in the solid wall, and γ is the ratio of the respective dielectric constants in the solid and liquid phases. In principle, this condition introduces a coupling to φ_s, itself governed by Laplace's equation within the solid wall and the continuity condition $\varphi_s = \varphi$ on S.

Other conditions necessary to fully specify the problem depend on the specific scenario considered. An important class of problems involves particulate motion in an unbounded fluid domain, where an additional set of condition is required "at infinity." These consist of a "driving" condition, representing the driver of the electrokinetic transport (e.g., an imposed electric field or concentration gradient) together with the specification of the far-field velocity profile [see (2.19)], reflecting the result of electrokinetic transport.

B. Prototypic example: electrophoresis

A prototypic example is the electrophoresis of a spherical particle (dimensional radius a^*) driven by a uniformly applied external field of dimensional magnitude E^*. The driving condition is

$$\nabla\varphi \to -\hat{\boldsymbol{\imath}}\beta \quad \text{as} \quad |\mathbf{x}| \to \infty. \tag{2.16}$$

Here $\hat{\boldsymbol{\imath}}$ a unit vector in the applied-field direction and

$$\beta = \frac{a^* E^*}{\varphi^*} \tag{2.17}$$

is the dimensionless field magnitude. In the absence of an imposed concentration gradient, both ionic concentrations approach a uniform concentration at large distances,

$$c^{\pm} \to 1 \quad \text{as} \quad |\mathbf{x}| \to \infty. \tag{2.18}$$

(This condition effectively defines c^*.) Finally, the velocity must approach the uniform incidence profile

$$\mathbf{u} \to -\mathscr{U}\hat{\boldsymbol{\imath}} \quad \text{as} \quad |\mathbf{x}| \to \infty, \tag{2.19}$$

wherein $\mathscr{U}$ is the magnitude of the particle electrophoretic velocity. This scalar quantity is to be found from the condition that the freely suspended particle is force free,

$$\oint_S dA\, \hat{\mathbf{n}} \cdot (\mathsf{N} + \mathsf{M}) = \mathbf{0}. \tag{2.20}$$

In view of Eq. (2.10), the integration domain may be chosen as any closed surface encapsulating the particle.

C. Weak fields

The classical analysis of O'Brien and White [7] entails an electrophoresis problem. While O'Brien and White formulated their problem using dimensional variables, inspection reveals that their weak-field approximation is tantamount to the assumption $\beta \ll 1$ in the present description; see (2.16)–(2.17). This issue deserves a clarification.

In section 3 of Ref. [7], O'Brien and White write "The difficulties involved in solving this set of coupled non-linear partial differential equations are formidable, but fortunately we are only concerned with the solution of these equations in the case when the applied field $\mathbf{E}$ is small compared with the fields that occur in the double layer." Since the Debye-layer voltage (the zeta potential) is comparable in magnitude to the thermal voltage φ^*, this implies fields that are small compared with $\kappa^*\varphi^*$. In the present dimensionless notation, this assumption reads $\delta\beta \ll 1$. Since Ref. [7] consider Debye thicknesses comparable to particle size, where $\delta \sim O(1)$, this is equivalent to $\beta \ll 1$.

When the Debye layer is thin, as in the follow-up analysis of O'Brien and Hunter [7], the two limits $\delta\beta \ll 1$ and $\beta \ll 1$ differ. It is, therefore, important to understand which of the two corresponds to the linearized equations in that paper. It is readily verified that the underlying limit is the more restrictive one, $\beta \ll 1$. For instance, the linearized equation set leaves out the (clearly nonlinear) term representing advection of ionic perturbations. Neglecting this term in the bulk region surrounding the double layer, where the relevant length scale is particle size rather than Debye thickness, is equivalent to assuming small β.

Our goal is to remove the restriction $\beta \ll 1$. In what follows, we generally allow for $\beta \sim O(1)$.

III. THIN-DOUBLE-LAYER LIMIT

We consider the thin-double-layer limit $\delta \to 0$. Poisson's equation (2.5) yields electro-neutrality

$$c^+ = c^- = c, \tag{3.1}$$

whereby the ionic fluxes (2.3) become

$$\mathbf{j}^\pm = \mp c\nabla\varphi - \nabla c. \tag{3.2}$$

Addition and subtraction of the Nersnt-Planck equations (2.2) respectively provide the salt concentration balance

$$\nabla^2 c = \frac{\alpha^+ + \alpha^-}{2}\mathbf{u}\cdot\nabla c \tag{3.3}$$

and charge balance

$$\nabla\cdot(c\nabla\varphi) = \frac{\alpha^+ - \alpha^-}{2}\mathbf{u}\cdot\nabla c. \tag{3.4}$$

Equations (2.8) and (2.9) are unaffected by the limit $\delta \to 0$; the Coulomb body forces in Eq. (2.9) originate from $O(\delta^2)$ volumetric charge density that is in general nonzero.

Note that the system (3.1)–(3.4) constitutes a leading-order description in a formal asymptotic expansion in $\delta \ll 1$. Moreover, this system is incompatible with the boundary conditions (2.14) and (2.15). This reflects the singular nature of the thin-double-layer limit, associated with the multiplication of the small expansion parameter by the highest derivative in Poisson's equation (2.5). Consequently, a boundary layer of $O(\delta)$ width develops about S, constituting the diffuse part of the double layer. In principle, asymptotic matching between the separate expansions in the electroneutral domain and the boundary layer provides effective boundary conditions for the former, resulting in a useful macroscale model. We denote the resulting "effective boundary" by s, to distinguish it from the literal interface S.

In the following section we will derive the effective boundary conditions for the classical case of moderate surface charge, where $\sigma \sim O(1)$.

IV. EFFECTIVE BOUNDARY CONDITIONS FOR MODERATELY CHARGED SURFACES

A. Boundary-layer formulation

In describing the diffuse layer we employ the method of Cox [29] (see also Ref. [50]), whereby points on S are identified by locally orthogonal curvilinear coordinates (ξ,η) possessing unity metric coefficients. Position normal to S is measured by a Cartesian coordinate z in the direction $\hat{\mathbf{e}}_\xi \times \hat{\mathbf{e}}_\eta$, pointing into the liquid, such that $z = 0$ on S. The boundary-layer scaling is implicit in the stretched normal coordinate

$$Z = z/\delta. \tag{4.1}$$

In the boundary-layer coordinates, the velocity field adopts the following Cartesian representation:

$$\mathbf{u} = \hat{\mathbf{e}}_\xi u + \hat{\mathbf{e}}_\eta v + \hat{\mathbf{e}}_z w. \tag{4.2}$$

Since both the ionic concentrations and electric potential are expected to be $O(1)$ within the boundary layer, we postulate the asymptotic expansions

$$c^\pm(\mathbf{x};\delta) = C_0^\pm(\xi,\eta,Z) + \cdots, \tag{4.3a}$$

$$\varphi(\mathbf{x};\delta) = \Phi_0(\xi,\eta,Z) + \cdots, \tag{4.3b}$$

together with similar scaling for the tangential components (u,v) of $\mathbf{u}$

$$u(\mathbf{x};\delta) = U_0(\xi,\eta,Z) + \cdots, \tag{4.4a}$$

$$v(\mathbf{x};\delta) = V_0(\xi,\eta,Z) + \cdots. \tag{4.4b}$$

From the continuity equation (2.8) and the impermeability condition (2.13) we then find that the normal velocity component is $O(\delta)$

$$w(\mathbf{x};\delta) = \delta W_1(\xi,\eta,Z) + \cdots. \tag{4.5}$$

Balancing the large Coulomb body forces in Eq. (2.9) then necessitates $O(\delta^{-2})$ pressure

$$p(\mathbf{x};\delta) = \delta^{-2}P_{-2}(\xi,\eta,Z) + \cdots. \tag{4.6}$$

In addition to Eqs. (4.3)–(4.6) we also introduce an asymptotic expansion for ionic fluxes in the z direction,

$$\hat{\mathbf{e}}_z\cdot\mathbf{j}^\pm = \delta^{-1}J_{-1}^\pm(\xi,\eta,Z) + J_0^\pm(\xi,\eta,Z) + \cdots. \tag{4.7}$$

Note that [see (2.3)]

$$J_{-1}^\pm = -\frac{\partial C_0^\pm}{\partial Z} \mp C_0^\pm\frac{\partial\Phi_0}{\partial Z}. \tag{4.8}$$

At large Z the boundary-layer variables must match the corresponding ones in the electro-neutral domain,

$$C_0^\pm \to c, \quad \Phi_0 \to \varphi, \quad V_0 \to v \quad \text{as} \quad Z \to \infty. \tag{4.9}$$

Hereafter, bulk-scale variables appearing in boundary-layer equations are understood to be evaluated on the effective boundary s and are, accordingly, functions of ξ and η alone. The matching requirement also implies that the following variables must vanish at large Z:

$$J_{-1}^\pm, P_{-2} \to 0 \quad \text{as} \quad Z \to \infty, \tag{4.10}$$

as, too, must the following derivatives:

$$\frac{\partial\Phi_0}{\partial Z}, \frac{\partial U_0}{\partial Z}, \frac{\partial V_0}{\partial Z} \to 0 \quad \text{as} \quad Z \to \infty. \tag{4.11}$$

The boundary conditions (2.13)–(2.15) applying on S must be rewritten in terms of the boundary-layer variables. Thus, the impermeability and no-slip condition (2.13) now

reads

$$U_0 = 0, \quad V_0 = 0, \quad W_1 = 0 \quad \text{at} \quad Z = 0, \tag{4.12}$$

the no-flux condition (2.14) implies

$$J^{\pm}_{-1} = 0, \quad J^{\pm}_{0} = 0, \quad \ldots \quad \text{at} \quad Z = 0, \tag{4.13}$$

and Gauss's condition (2.15) becomes

$$\frac{\partial \Phi_0}{\partial Z} = -\sigma \quad \text{at} \quad Z = 0, \tag{4.14}$$

where the electric displacement in the solid phase (within which no boundary layer develops) is relegated to a higher-order balance.

B. Boundary-layer analysis

At $O(\delta^{-2})$ the ionic balances (2.2) yield

$$\frac{\partial J^{\pm}_{-1}}{\partial Z} = 0, \tag{4.15}$$

which, together with Eq. (4.10), imply $J^{\pm}_{-1} \equiv 0$. Use of Eq. (4.8) in conjunction with Eq. (4.9) provides the Boltzmann distributions

$$C^{\pm}_0 = c\, e^{\mp \Psi} \tag{4.16}$$

wherein

$$\Psi = \Phi_0 - \varphi \tag{4.17}$$

is the "excess" boundary-layer potential. Substitution into Poisson's equation (2.5) yields, at leading order,

$$\frac{\partial^2 \Psi}{\partial Z^2} = c \sinh \Psi. \tag{4.18}$$

Integration in conjunction with Eq. (4.11) yields

$$\frac{\partial \Psi}{\partial Z} = -2\sqrt{c} \sinh \frac{\Psi}{2}. \tag{4.19}$$

A subsequent integration furnishes the Gouy-Chapman distribution

$$\tanh \frac{\Psi}{4} = e^{-Z\sqrt{c}} \tanh \frac{\zeta}{4}, \tag{4.20}$$

where the dimensionless "zeta potential"

$$\zeta(\xi,\eta) = \Psi(\xi,\eta,0) \tag{4.21}$$

is the boundary-layer voltage. In view of Eqs. (4.14) and (4.19), the zeta potential depends on the prescribed surface charge density through the relation

$$\sigma = 2\sqrt{c} \sinh \frac{\zeta}{2}. \tag{4.22}$$

While σ is uniform, ζ is generally not so.

In calculating the flow we follow Rubinstein and Zaltzman [30]. With Ψ known, the pressure field P_{-2} is obtained from the leading-order momentum balance in the z direction [see (2.9)],

$$\frac{\partial P_{-2}}{\partial Z} = \frac{\partial^2 \Phi_0}{\partial Z^2} \frac{\partial \Phi_0}{\partial Z}. \tag{4.23}$$

Integration in conjunction with Eq. (4.10) readily yields

$$P_{-2} = \frac{1}{2} \left(\frac{\partial \Psi}{\partial Z} \right)^2. \tag{4.24}$$

The leading-order momentum balance in the ξ direction [see (2.9)] reads

$$\frac{\partial P_{-2}}{\partial \xi} = \frac{\partial^2 U_0}{\partial Z^2} + \frac{\partial^2 \Phi_0}{\partial Z^2} \frac{\partial \Phi_0}{\partial \xi}. \tag{4.25}$$

Substitution of Eq. (4.24) in conjunction with the definition (4.17) yields

$$\frac{\partial^2 U_0}{\partial Z^2} = \frac{\partial \Psi}{\partial Z} \frac{\partial^2 \Psi}{\partial Z\, \partial \xi} - \frac{\partial^2 \Psi}{\partial Z^2} \left(\frac{\partial \Psi}{\partial \xi} + \frac{\partial \varphi}{\partial \xi} \right). \tag{4.26}$$

Use of Eq. (4.19) allows one integration of this differential equation,

$$\frac{\partial U_0}{\partial Z} = -\frac{\partial \Psi}{\partial Z} \frac{\partial \varphi}{\partial \xi} - \frac{4}{\sqrt{c}} \frac{\partial c}{\partial \xi} \sinh^2 \frac{\Psi}{4}, \tag{4.27}$$

where the constant of integration must vanish in view of Eq. (4.11). Substitution of Eq. (4.20) allows for yet another integration, which, in conjunction with the no-slip condition (4.12) and definition (4.21), yields

$$U_0 = (\zeta - \Psi) \frac{\partial \varphi}{\partial \xi} + 2 \ln \frac{1 - \tanh^2 \frac{\zeta}{4}}{1 - e^{-2Z\sqrt{c}} \tanh^2 \frac{\zeta}{4}} \frac{\partial \ln c}{\partial \xi}. \tag{4.28}$$

A similar expression, involving derivatives with respect to η, holds for V_0. The first term in Eq. (4.28) originates from the action of Coulomb body forces on the charged fluid elements within the diffuse layer, while the second term stems from nonequlibrium tangential pressure variations (in the ξ and η directions) associated with concentration gradients.

Finally, we consider the $O(\delta^{-1})$ balance of the ionic conservation equations (2.2). At this asymptotic order the advection term still does not contribute, and we get

$$\frac{\partial J^{\pm}_0}{\partial Z} + (\nabla \cdot \hat{\mathbf{n}}) J^{\pm}_{-1} = 0, \tag{4.29}$$

where the second term, proportional to the local curvature of S, is associated with the curvilinear nature of the (ξ,η) coordinates (see Ref. [29]). Given the vanishing of $J^{\pm}_{-1}$ this term disappears as well, eventually giving

$$\frac{\partial J^{\pm}_0}{\partial Z} = 0. \tag{4.30}$$

The no-flux condition (4.13) then implies that

$$J^{\pm}_0 \equiv 0. \tag{4.31}$$

C. Effective boundary conditions

We can now obtain effective boundary conditions using asymptotic matching between the boundary-layer fields and their counterparts in the electroneutral domain. Consider, first, the velocity field. The 1–1 van Dyke matching rule [27] in conjunction with the inner scaling (4.5) of the normal velocity readily yields

$$w = 0 \quad \text{on} \quad s. \tag{4.32}$$

The boundary conditions governing the tangential components are obtained from Eq. (4.9). Evaluation of Eq. (4.28) at the outer edge of the boundary layer, $Z \to \infty$, yields the familiar Dukhin-Derjaguin slip condition,

$$u = \zeta \frac{\partial \varphi}{\partial \xi} + 2 \ln \left(1 - \tanh^2 \frac{\zeta}{4} \right) \frac{\partial \ln c}{\partial \xi} \quad \text{on} \quad s. \tag{4.33}$$

A similar condition applies for v.

Consider now the ionic fluxes normal to s in the electroneutral domain, $\hat{\mathbf{n}} \cdot \mathbf{j}^{\pm}$, which adopt the respective forms [see (3.2)]

$$-c \frac{\partial \varphi}{\partial n} - \frac{\partial c}{\partial n}, \quad c \frac{\partial \varphi}{\partial n} - \frac{\partial c}{\partial n}. \tag{4.34}$$

Asymptotic matching with the null $O(1)$ ionic fluxes (4.31) readily yields the homogenous Neumann conditions

$$\frac{\partial \varphi}{\partial n} = 0, \quad \frac{\partial c}{\partial n} = 0 \quad \text{on} \quad s. \tag{4.35}$$

V. BREAKUP FOR HIGHLY CHARGED SURFACES

A. Large zeta potentials: The emergence of an internal boundary layer

The preceding macroscale model breaks up for highly charged surfaces when ζ is large [see (4.22)]. Indeed, consider (with no loss of generality) the case of positive σ. Because of the Boltzmann distribution (4.16) the anion concentration near the surface is $O(e^{\zeta})$ large. It follows that, at sufficiently large zeta potentials, tangential ionic fluxes emerge at the ionic transport balance (4.29), resulting in a significant transverse flux normal to the surface.

These tangential fluxes are essentially confined to a small portion of the Debye-layer cross section, adjacent to the charged surface. In this region, where the charge density is large, Poisson's equation (2.5) implies steep transverse gradients in the electric potential, above and beyond the $O(\delta^{-1})$ values appropriate to moderate zeta potentials. Indeed, with the surface-charge density σ being $O(e^{\zeta/2})$ [see (4.22)], Gauss's condition implies transverse electric fields of order $\delta^{-1} e^{\zeta/2}$ near the surface. As the (counterion dominated) volumetric charge density is $O(e^{\zeta})$ in this region, Poisson's equation then provides the transverse length scale

$$\delta e^{-\zeta/2} \tag{5.1}$$

(much smaller than the Debye thickness δ) on which the electric field must vary so as to account for the high charge density.

With the length scale (5.1) available, we can now estimate the asymptotic magnitude of the transverse anionic flux. Due to the large anionic concentration, the ionic fluxes in the tangential (ξ, η) directions are of order e^{ζ}. The net fluxes through an $O(\delta e^{-\zeta/2})$-wide cross section are, therefore, of order $\delta e^{\zeta/2}$ and so are their respective surface derivatives. The ionic transport balance (4.29) then necessitates a transverse flux of the same asymptotic magnitude. The moderate-surface-charge model will accordingly break down when the zeta potential is "logarithmically large,"

$$\delta e^{\zeta/2} \sim O(1). \tag{5.2}$$

At these moderately large ζ values the transverse flux becomes $O(1)$, negating the nil result (4.31) which has been obtained for moderate zeta potentials

From Eqs. (5.1) and (5.2) it then follows that the surface conduction region is of $O(\delta^2)$ thickness. This motivates the introduction, at highly charged surfaces ($\sigma \gg 1$), of an *internal* boundary layer of that thickness near the solid surface. We refer to this newly defined asymptotic region—originally mentioned by Hinch *et al.* [12]—as the "Dukhin layer." We hereafter refer to the "Debye layer" as the diffuse layer after the Dukhin sublayer has been conceptually removed. In the limit of highly charged surface the counterion concentration thus shifts from $O(1)$ values at the Debye layer to $O(\delta^{-2})$ values in the Dukhin layer. This corresponds to a comparable transition of the tangential counterion flux.

In deriving the macroscale model appropriate for the limit process (5.4) we accordingly analyze these asymptotic regions separately. This eliminates the nonrigorous procedure where formally asymptotically small terms are retained at the leading-order balances. Note that the excess potential is moderate in the Debye layer and is $O(\ln \delta)$ in the Dukhin sublayer. Following the conventional asymptotic methodology [31], these asymptotic orders are considered on the same par.

B. Dimensionless number

When defining a dimensionless number representing the transition to the high-charge limit, Eq. (5.2) naturally suggest it as the product $\delta e^{\zeta/2}$ (related to the familiar definition of the Dukhin number). In that limit, however, the zeta potential is *inherently nonuniform*, exactly because of the transverse ionic flux animated by surface conduction: This flux gives rise to salt concentration polarization, rendering the zeta potential nonuniform even when the surface charge density is uniform (as we assume here for simplicity)—see (4.22). To define a *global* parameter, we need to identify a *constant* quantity that scales essentially as $e^{\zeta/2}$; equivalently [see (5.2)], it should be $O(1)$ for moderately charged surfaces but become $O(\delta^{-1})$ for highly charged surfaces.

This quantity is simply given by the surface charge σ, as is evident from Eqs. (2.15) and (5.2). We therefore define the Bikerman number as

$$\mathrm{Bi} = \delta \sigma. \tag{5.3}$$

The high-charge limit is, therefore, described by the limit process

$$\delta \to 0 \quad \text{with} \quad \mathrm{Bi} \sim O(1). \tag{5.4}$$

The moderate-charge limit, derived in Sec. IV assuming $\sigma \sim O(1)$, corresponds to $\mathrm{Bi} \sim O(\delta)$. The asymptotic regimes associated with different values of the zeta potential are depicted in Fig. 1. The critical Bikerman number $\mathrm{Bi}_{\mathrm{cr}}$, and the appearance of nondilute effects at $\mathrm{Bi} \gtrsim \mathrm{Bi}_{\mathrm{cr}}$, are discussed in Sec. VII.

In deriving the high-charge limit, it is actually convenient to employ a *characteristic* zeta potential $\bar{\zeta}$, defined via the relation [see (4.22)]

$$\sigma = e^{\bar{\zeta}/2}. \tag{5.5}$$

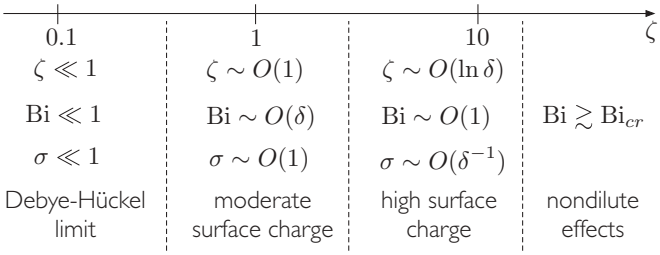

FIG. 1. A schematic decomposition of the various asymptotic regimes associated with different values of ζ.

The Bikerman number is given by the more "familiar" notation

$$\mathrm{Bi} = \delta e^{\bar{\zeta}/2}. \tag{5.6}$$

In view of Eq. (4.22), $\bar{\zeta}$ represents the zeta-potential values attained over highly charged surface.

We conclude that at $O(1)$ Bikerman numbers, one needs to separately solve the governing equations in three asymptotic domains: the electroneutral domain, the $O(\delta)$-wide Debye layer, and the $O(\delta^2)$-wide Dukhin layer. The spatial decomposition into these three regions in the limit (5.4) is schematically portrayed in Fig. 2. The electroneutral description, provided by (2.8) and (2.9), and (3.3) and (3.4), is unaffected by the transition to the limit process (5.4). On the other hand, part of the boundary-layer analysis in Sec. IV has used the boundary conditions on S, which now do not apply to the Debye-layer fields but rather to those of the Dukhin sublayer. Thus, Debye-layer fields must now be determined via asymptotic matching with the corresponding variables in *both* the electroneutral domain and the Dukhin sublayer, while the latter must be solved separately using the condition on S. This procedure, eventually leading to a different set of effective conditions on s replacing (4.33)–(4.35) is performed in the next section.

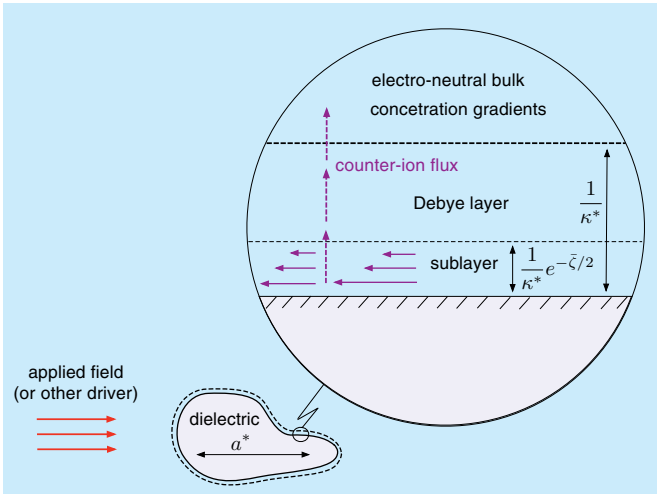

FIG. 2. (Color online) Asymptotic decomposition of the fluid domain in the limit $\delta \to 0$ for $\mathrm{Bi} \sim O(1)$. Nonuniformities in the tangential counterion fluxes within the Dukhin layer result in $O(1)$ normal fluxes which cross the Debye layer into the electroneutral bulk.

VI. DEBYE-LAYER AND DUKHIN-LAYER ANALYSES FOR HIGHLY CHARGED SURFACES

A. Debye-layer analysis

In the present context, the Debye-layer formulation is still provided by Eq. (4.1)–(4.11), but (4.12)–(4.14), derived from the microscale conditions on S, no longer apply. Consequently, the analysis (4.15)–(4.19) remains valid, whereby (4.20) is replaced by

$$\tanh\frac{\Psi}{4} = A(\xi,\eta)e^{-Z\sqrt{c}} \tag{6.1}$$

in which the integration constant A is to be obtained from asymptotic matching with the Dukhin sublayer. Similarly, the momentum analysis (4.23)–(4.27) remains valid, but it no longer leads to Eq. (4.28), which hinges upon the no-slip condition. Rather, integration of Eq. (4.27) from Z to ∞ yields

$$u - U = \Psi\frac{\partial\varphi}{\partial\xi} - \frac{4}{\sqrt{c}}\frac{\partial c}{\partial\xi}\int_Z^\infty \sinh^2\frac{\Psi(t)}{4}\,dt. \tag{6.2}$$

The integral in this expression is readily evaluated using (4.19). This provides the present counterpart of Eq. (4.28)

$$u - U = \Psi\frac{\partial\varphi}{\partial\xi} - \frac{4}{c}\frac{\partial c}{\partial\xi}\ln\cosh\frac{\Psi}{4}, \tag{6.3}$$

where the "integration constant" u—the electro-neutral slip on s—is to be found from asymptotic matching with the sublayer.

Finally, Eqs. (4.29)–(4.30) also retain their validity, whence $J_0^{\pm}$ is a constant (i.e., a function of ξ and η alone), but (4.31) is not necessarily valid; $J_0^{\pm}$ may be nonzero. Clearly, with the no-flux condition on the solid wall and the constancy of $J_0^{\pm}$ in the Debye layer, any such nonzero transverse flux must originate in the Dukhin layer.

B. Dukhin-layer formulation

Following the scaling analysis of Sec. V we define the Dukhin-layer coordinate [cf. (4.1)]

$$\tilde{Z} = z/\delta^2 = Z/\delta. \tag{6.4}$$

In view of the Boltzmann distributions (4.16) and the scaling (5.2), it is anticipated that the anionic concentration in the sublayer is $O(\delta^{-2})$

$$c^-(\mathbf{x};\delta) = \delta^{-2}\tilde{C}^-_{-2}(\xi,\eta,\tilde{Z}) + \cdots, \tag{6.5}$$

while the cation concentration is $O(\delta^2)$.

When dealing with asymptotic expansions in algebraic powers of a small parameter, logarithmic terms are considered $O(1)$ [31]. We therefore postulate for the electric potential,

$$\varphi(\mathbf{x};\delta) = \tilde{\Phi}_0(\xi,\eta,\tilde{Z}) + \cdots. \tag{6.6}$$

Similarly to Eq. (4.17), we define the excess potential $\tilde{\Psi}$ via the relation

$$\tilde{\Phi}_0 = \varphi + \tilde{\Psi}, \tag{6.7}$$

where, in the usual manner, φ denotes the value of the bulk potential just outside the Debye layer. In addition, we decompose $\tilde{\Psi}$ in the form

$$\tilde{\Psi} = \zeta + \Gamma \tag{6.8}$$

wherein ζ (a function of ξ of η alone) is defined such that

$$\Gamma(\tilde{Z}=0)=0. \tag{6.9}$$

Thus, ζ retains the interpretation of the leading-order voltage drop on the entire Debye layer (including the sublayer). As will become evident, the voltage Γ, as defined in Eq. (6.8), is a function of $\tilde{Z}$ alone, independent of ξ of η.

In view of the momentum balance (2.9) in the normal direction we anticipate an $O(\delta^{-4})$ large pressure in the sublayer,

$$p=\delta^{-4}\tilde{P}_{-4}+\cdots. \tag{6.10}$$

We still postulate $O(1)$ tangential velocities

$$u=\tilde{U}_0+\cdots, \quad v=\tilde{V}_0+\cdots, \tag{6.11}$$

whereby the continuity equation (2.8) and the impermeability condition (2.13) in conjunction with the scaling (6.4) suggest an $O(\delta^2)$ normal velocity,

$$w=\delta^2\tilde{W}_2+\cdots. \tag{6.12}$$

The required matching of the normal anionic flux in the sublayer with that in the Debye layer in conjunction with Eq. (4.30) implies that this flux must actually match the corresponding one in the electroneutral region. We, therefore, anticipate an $O(1)$ anionic flux,

$$\hat{\mathbf{e}}_z\cdot\mathbf{j}^-=\tilde{J}_0^-+\cdots. \tag{6.13}$$

On the other hand, the large anionic concentration suggests large anionic fluxes in the tangential directions,

$$(\mathbf{I}-\hat{\mathbf{e}}_z\hat{\mathbf{e}}_z)\cdot\mathbf{j}^-=\delta^{-2}\tilde{\mathbf{J}}_{-2}^-+\cdots; \tag{6.14}$$

here substitution of Eq. (2.3) yields

$$\tilde{\mathbf{J}}_{-2}^-=-\boldsymbol{\nabla}_\parallel\tilde{C}_{-2}^-+\tilde{C}_{-2}^-\boldsymbol{\nabla}_\parallel\tilde{\Phi}_0 \tag{6.15}$$

in which

$$\boldsymbol{\nabla}_\parallel=\hat{\mathbf{e}}_\xi\frac{\partial}{\partial\xi}+\hat{\mathbf{e}}_\eta\frac{\partial}{\partial\eta} \tag{6.16}$$

is the projection of the gradient operator in the tangential direction.

At large $\tilde{Z}$ the sublayer fields must match the small-Z expansions of the corresponding Debye fields. In addition, they must satisfy at $\tilde{Z}=0$ the appropriate boundary condition on S. The impermeability and no-slip condition (2.13) now reads

$$\tilde{U}_0=\tilde{V}_0=\tilde{W}_2=0 \quad \text{at} \quad \tilde{Z}=0. \tag{6.17}$$

In view of the no-flux condition (2.14), the $O(1)$ anionic flux normal to S must vanish,

$$\tilde{J}_0^-=0 \quad \text{at} \quad \tilde{Z}=0. \tag{6.18}$$

Finally, using (6.6)–(6.8) together with Eqs. (5.5) and (5.6), we obtain from Gauss's law (2.15) in terms of the stretched variable (6.4),

$$\frac{\partial\Gamma}{\partial\tilde{Z}}=-\mathrm{Bi} \quad \text{at} \quad \tilde{Z}=0. \tag{6.19}$$

C. Dukhin-layer analysis

Since the anionic flux in the z direction begins at $O(1)$ [see Eq. (6.13)] the term

$$-\frac{\partial\tilde{C}_{-2}^-}{\partial\tilde{Z}}+\tilde{C}_{-2}^-\frac{\partial\Gamma}{\partial\tilde{Z}}, \tag{6.20}$$

representing $O(\delta^{-4})$ flux, must vanish; this, in conjunction with Eq. (5.6), results in the Boltzmann distribution

$$\tilde{C}_{-2}^-=c\,\mathrm{Bi}^2e^{\zeta-\bar{\zeta}}e^{\Gamma}, \tag{6.21}$$

wherein matching between Dukhin-layer and Debye-layer fields is already accounted for.

Consider now Poisson's equation (2.5) at $O(\delta^{-2})$,

$$2\frac{\partial^2\Gamma}{\partial\tilde{Z}^2}=\tilde{C}_{-2}^-. \tag{6.22}$$

Substitution of Eq. (6.21), multiplication by $\partial\Gamma/\partial\tilde{Z}$, and integration yields

$$\left(\frac{\partial\Gamma}{\partial\tilde{Z}}\right)^2=c\,\mathrm{Bi}^2e^{\zeta-\bar{\zeta}}e^{\Gamma}+B(\xi,\eta). \tag{6.23}$$

Since $\partial\Gamma/\partial\tilde{Z}$ and e^{Γ} are respectively proportional to the $O(\delta^{-2})$ transverse electric field and anionic concentration within the Dukhin layer, they must vanish at large $\tilde{Z}$ due to the different scaling of these fields in the Debye layer. Thus, $B=0$:

$$\frac{\partial\Gamma}{\partial\tilde{Z}}=-\mathrm{Bi}\sqrt{c\,e^{\zeta-\bar{\zeta}}e^{\Gamma}}. \tag{6.24}$$

Application of Eq. (6.19) then reveals the following relation between $\zeta-\bar{\zeta}$ and the bulk concentration c,

$$c\,e^{\zeta-\bar{\zeta}}=1, \tag{6.25}$$

resulting in the simplified first-order equation

$$\frac{\partial\Gamma}{\partial\tilde{Z}}=-\mathrm{Bi}\,e^{\Gamma/2}. \tag{6.26}$$

Integration of Eq. (6.26) in conjunction with Eq. (6.9) yields (cf. Ref. [8])

$$\Gamma=2\ln\frac{2}{2+\mathrm{Bi}\tilde{Z}}; \tag{6.27}$$

note that Γ is a function of $\tilde{Z}$ alone. Matching with Eq. (6.1) then reveals that $A=1$, providing the excess-potential distribution in the Debye layer

$$\Psi=2\ln\frac{1+e^{-Z\sqrt{c}}}{1-e^{-Z\sqrt{c}}}. \tag{6.28}$$

Unsurprisingly, this distribution represents the large-ζ limit of the Gouy-Chapman distribution (4.20).

We note that (6.25) implies the following ζ distribution:

$$\zeta=\bar{\zeta}-\ln c \tag{6.29}$$

or, using (5.6),

$$\zeta=2\ln\frac{\mathrm{Bi}}{\delta\sqrt{c}}; \tag{6.30}$$

in addition, it simplifies (6.21) to

$$\tilde{C}_{-2}^-=\mathrm{Bi}^2e^{\Gamma}. \tag{6.31}$$

Remarkably, $\tilde{C}^-_{-2}$ is independent of ξ and η. Substitution of (6.7) and (6.8) together with Eqs. (6.29) and (6.31) into (6.15) yields,

$$\tilde{\mathbf{J}}^-_{-2} = \mathrm{Bi}^2 e^{\Gamma} \boldsymbol{\nabla}_{\parallel}(\varphi - \ln c). \tag{6.32}$$

Since the anions do not satisfy a Boltzmann distribution in the electroneutral region, the gradient of their chemical potential $\varphi - \ln c$ does not necessarily vanish; hence, $\tilde{\mathbf{J}}^-_{-2}$ is generally nonzero.

Consider now the momentum balance (2.9). In the normal direction at $O(\delta^{-5})$ we find the equation [cf. (4.23)]

$$\frac{\partial \tilde{P}_{-4}}{\partial \tilde{Z}} = \frac{\partial^2 \Gamma}{\partial \tilde{Z}^2}\frac{\partial \Gamma}{\partial \tilde{Z}}, \tag{6.33}$$

whose solution is

$$\tilde{P}_{-4} = \frac{1}{2}\left(\frac{\partial \Gamma}{\partial \tilde{Z}}\right)^2, \tag{6.34}$$

where the constant of integration vanishes due to asymptotic matching with the $O(\delta^{-2})$ Debye-layer pressure, when use is made of the large-$\tilde{Z}$ decay of $\partial\Gamma/\partial\tilde{Z}$.

In the ξ direction, at $O(\delta^{-4})$, the momentum balance (2.9) yields [cf. (4.25)]

$$\frac{\partial \tilde{P}_{-4}}{\partial \xi} = \frac{\partial^2 \tilde{U}_0}{\partial \tilde{Z}^2} + \frac{\partial^2 \tilde{\Phi}_0}{\partial \tilde{Z}^2}\frac{\partial \tilde{\Phi}_0}{\partial \xi}. \tag{6.35}$$

Substitution of Eq. (6.34) in conjunction with the definitions (6.7) and (6.8) yields

$$\frac{\partial^2 \tilde{U}_0}{\partial \tilde{Z}^2} = \frac{\partial \Gamma}{\partial \tilde{Z}}\frac{\partial^2 \Gamma}{\partial \xi \partial \tilde{Z}} - \frac{\partial^2 \Gamma}{\partial \tilde{Z}^2}\frac{\partial}{\partial \xi}(\varphi + \zeta + \Gamma). \tag{6.36}$$

Since Γ is independent of ξ, integration yields

$$\frac{\partial \tilde{U}_0}{\partial \tilde{Z}} = -\frac{\partial \Gamma}{\partial \tilde{Z}}\frac{\partial}{\partial \xi}(\varphi + \zeta). \tag{6.37}$$

where the constant of integration vanishes due to asymptotic matching with the Debye-scale velocity. One more integration, in conjunction with Eq. (6.9) and the no-slip condition (6.17), furnishes the velocity profile

$$\tilde{U}_0 = -\Gamma \frac{\partial}{\partial \xi}(\varphi + \zeta). \tag{6.38}$$

A similar expression holds for $\tilde{V}_0$. In vector notation,

$$\tilde{\mathbf{U}}_0 = -\Gamma \boldsymbol{\nabla}_{\parallel}(\varphi + \zeta), \tag{6.39}$$

wherein $\tilde{\mathbf{U}}_0$ is the tangential projection of the velocity vector [cf. (6.14)]

$$\tilde{\mathbf{U}}_0 = \hat{\mathbf{e}}_{\xi}\tilde{U}_0 + \hat{\mathbf{e}}_{\eta}\tilde{V}_0. \tag{6.40}$$

Finally, consider the anionic balance (2.2) at $O(\delta^{-2})$:

$$\frac{\partial \tilde{J}^-_0}{\partial \tilde{Z}} + \boldsymbol{\nabla}_{\parallel}\cdot\tilde{\mathbf{J}}^-_{-2} + \alpha^-\left(\tilde{\mathbf{U}}_0\cdot\boldsymbol{\nabla}_{\parallel}\tilde{C}^-_{-2} + \tilde{W}_2\frac{\partial \tilde{C}^-_{-2}}{\partial \tilde{Z}}\right) = 0. \tag{6.41}$$

Integration over $\tilde{Z}$ in conjunction with Eq. (6.18) yields

$$-\tilde{J}^-_0(\tilde{Z}\to\infty) = \boldsymbol{\nabla}_{\parallel}\cdot\int_0^{\infty}\tilde{\mathbf{J}}^-_{-2}\,d\tilde{Z} + \alpha^-\int_0^{\infty}\left(\tilde{\mathbf{U}}_0\cdot\boldsymbol{\nabla}_{\parallel}\tilde{C}^-_{-2} + \tilde{W}_2\frac{\partial \tilde{C}^-_{-2}}{\partial \tilde{Z}}\right)d\tilde{Z}, \tag{6.42}$$

where in the first term on the right-hand side we have interchanged the order of transverse integration and tangential differentiation. Substitution of Eq. (6.27) into (6.32) followed by integration yields for this term

$$2\mathrm{Bi}\nabla_s^2(\varphi - \ln c). \tag{6.43}$$

Consider now the second term on the right-hand side. Making use of the leading-order continuity equation

$$\boldsymbol{\nabla}_{\parallel}\cdot\tilde{\mathbf{U}}_0 + \frac{\partial \tilde{W}_2}{\partial \tilde{Z}} = 0, \tag{6.44}$$

yields, via integration by parts,

$$\int_0^{\infty}\tilde{W}_2\frac{\partial \tilde{C}^-_{-2}}{\partial \tilde{Z}}\,d\tilde{Z} = [\tilde{W}_2\tilde{C}^-_{-2}]^{\infty}_{\tilde{Z}=0} + \int_0^{\infty}\tilde{C}^-_{-2}\boldsymbol{\nabla}_{\parallel}\cdot\tilde{\mathbf{U}}_0\,d\tilde{Z}. \tag{6.45}$$

The boundary terms vanish at both $\tilde{Z}=0$ [due to (6.17)] and $\tilde{Z}\to\infty$ (since the decay of $\tilde{C}^-_{-2}$ as $\tilde{Z}^{-2}$ dominates over the $\sim\tilde{Z}\ln\tilde{Z}$ divergence of $\tilde{W}_2$). It follows that the second term on the right-hand side of Eq. (6.42) is

$$\alpha^-\int_0^{\infty}\boldsymbol{\nabla}_{\parallel}\cdot(\tilde{C}^-_{-2}\tilde{\mathbf{U}}_0)\,d\tilde{Z} = \alpha^-\boldsymbol{\nabla}_{\parallel}\cdot\int_0^{\infty}\tilde{C}^-_{-2}\tilde{\mathbf{U}}_0\,d\tilde{Z}.$$

Substitution of Eqs. (6.31) and (6.39) followed by integration using (6.27) finally yields for this term

$$4\alpha^-\mathrm{Bi}\nabla_s^2(\varphi - \ln c). \tag{6.46}$$

Using (6.43) and (6.46) we conclude that

$$\tilde{J}^-_0(\tilde{Z}\to\infty) = -2\mathrm{Bi}(1+2\alpha^-)\nabla_s^2(\varphi - \ln c). \tag{6.47}$$

Because of the low cationic concentration, it readily follows that the cationic flux at this order vanishes identically (as in the case of moderate surface charge).

D. *A posteriori* verification

In defining the Bikerman number, we have sought a constant quantity which scales as $\exp(\zeta/2)$. Scaling arguments have suggested the use of σ, the dimensionless surface-charge density. The "characteristic" zeta potential $\bar{\zeta}$ was accordingly defined through $\sigma = \exp(\bar{\zeta}/2)$. Indeed, in the following analysis we have tacitly assumed that a term like $e^{\zeta-\bar{\zeta}}$, which appears throughout the Dukhin-layer analysis [see, e.g., (6.21)], is of order unity even though each of the exponents alone is asymptotically large.

Our analysis provides an *a posteriori* verification to this underlying assumption. Indeed, it eventually leads to relation (6.25) which alternatively reads

$$e^{\bar{\zeta}/2} = c^{1/2}e^{\zeta/2}. \tag{6.48}$$

Since c is $O(1)$, this relation justifies our scaling procedure.

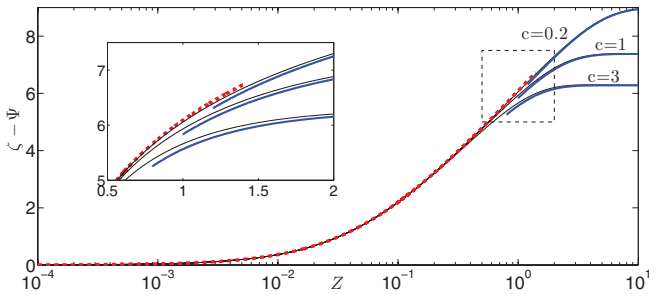

FIG. 3. (Color online) Relative potential $\zeta - \Psi$ as a function of Z for Bi $= 0.4$, $\delta = 0.01$, and the indicated values of c. The dashed curve represents the Dukhin-layer approximation, obtained from Eq. (6.27). The solid lines represent the Debye-layer approximation, obtained from Eq. (6.28). The thin lines represent the uniform approximation, where Ψ is provided by Eq. (6.49). The inset is a zoom of the matching region, marked by the dashed box.

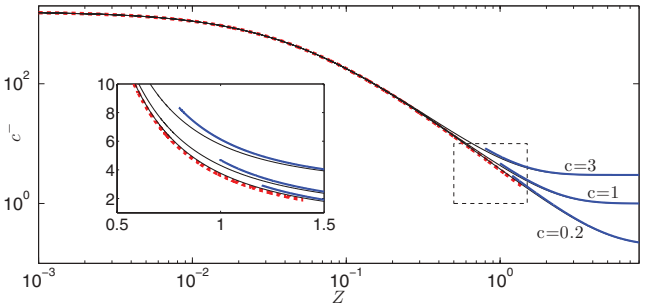

FIG. 4. (Color online) Counterion concentration c^- as a function of Z for Bi $= 0.4$, $\delta = 0.01$, and the indicated values of c. The dashed curve represents the Dukhin-layer approximation (6.50), the solid lines represent the Debye-layer approximation (6.51), and the thin lines represent the uniform approximation. The inset is a zoom of the matching region, marked by the dashed box.

E. Universal structure

A peculiar feature of the Dukhin layer is the independence of Γ on the concentration value c at the outer edge of the Debye layer; see (6.27). Recalling that Γ represents the potential relative to the wall [see (6.8)], it corresponds to the potential difference $\Psi - \zeta$ in the Debye layer. In that region, this potential difference does depend on c; see (6.28).

The universal structure of the relative potential in the Dukhin layer is illustrated in Fig. 3, where $\zeta - \Psi$ is plotted against the Debye-scale coordinate Z for Bi $= 0.4$ and $\delta = 0.01$ [corresponding to $\bar{\zeta} \approx 7.4$; see (5.6)]. Three values for c (0.2, 1, and 3) are chosen for the illustration, conceptually corresponding to different points (ξ,η) on the highly charged surface (with $c = 1$ representing the entire surface in the absence of salt polarization); these local concentrations correspond to $\zeta \approx 9$, $\zeta = \bar{\zeta}$, and $\zeta \approx 6.3$; see (6.29). The dashed line delineates the Dukhin-layer approximation $-\Gamma$, obtained from Eq. (6.27). The solid curves represent the respective Debye-layer approximations, obtained from Eq. (6.28). Also shown (thin lines) are the corresponding uniform approximations, in which Ψ is approximated in the usual fashion [32] by adding the respective Dukhin- and Debye-layer approximations and subtracting their common part, $2\ln(2/Z\sqrt{c})$. Using (5.3) and (6.30), this approximation reads

$$\Psi \approx 2\ln\frac{\mathrm{Bi}\tilde{Z}}{2+\mathrm{Bi}\tilde{Z}} + 2\ln\frac{1+e^{-Z\sqrt{c}}}{1-e^{-Z\sqrt{c}}}. \tag{6.49}$$

Even more remarkable is the c-independent structure of the counterion concentration in the Dukhin layer; see (6.27). This is in sharp contrast with the counterion concentration in the Debye layer, which clearly depends on the bulk concentration c [see (4.9) and (4.16)]. The universal Dukhin-layer structure is illustrated in Fig. 4, again using the values Bi $= 0.4$ and $\delta = 0.01$ and the bulk-concentration values 0.2, 1, and 3. The dashed curve represents the leading-order Dukhin-layer approximation [see (6.5), (6.27), and (6.31)]

$$\delta^{-2}\mathrm{Bi}^2\left(\frac{2}{2+\mathrm{Bi}\tilde{Z}}\right)^2, \tag{6.50}$$

the solid curves describe the leading-order Debye-layer approximation [see (4.16) and (6.28)]

$$c\left(\frac{1+e^{-Z\sqrt{c}}}{1-e^{-Z\sqrt{c}}}\right)^2, \tag{6.51}$$

and the thin curves delineate the corresponding uniform approximation, evaluated via addition of Eqs. (6.50) and (6.51) and subtraction of the common part, $4/Z^2$.

F. Effective boundary conditions

In deriving effective boundary conditions we consider, first, the velocity field. Condition (4.32), based on the scaling of the normal velocity within the Debye layer, is unaffected by the presence of the Dukhin sublayer. The slip condition (4.33), however, is modified. Thus, asymptotic matching between (6.38) and the Debye-scale profile (6.3) yields here

$$u = 4\ln 2\frac{\partial}{\partial\xi}\ln c + \zeta\frac{\partial}{\partial\xi}(\varphi - \ln c); \tag{6.52}$$

a similar expression holds for the velocity component v in the η direction.

Consider now the $O(1)$ ionic fluxes normal to the surface. In view of Eq. (4.30), the fluxes in the Dukhin layer must directly match the electroneutral fluxes (4.34). The nil cationic flux in the sublayer readily yields the homogeneous condition

$$\frac{\partial c}{\partial n} + c\frac{\partial\varphi}{\partial n} = 0, \tag{6.53}$$

which also applies at moderate surface charge; see (4.34). On the other hand, matching of the anionic flux (6.47) provides the inhomogeneous condition

$$\frac{\partial c}{\partial n} = \mathrm{Bi}(1+2\alpha^-)\nabla_s^2(\varphi - \ln c), \tag{6.54}$$

which constitutes the main macroscale manifestation of surface conduction.

VII. SURFACE CONDUCTION VERSUS NONDILUTE EFFECTS: DOMINANT MECHANISM AT LARGE ZETA POTENTIALS?

Surface conduction emerges at large zeta potentials due to the intense counterion concentration near the charge solid-liquid interface. As the counterion concentration is intensified in that region, ion-ion interactions may become appreciable as well. Just as surface conduction, these interactions modify the classical electrokinetic description. The latter modification, however, takes place at a more fundamental level, implying the eventual breakdown of the underlying Poisson-Nernst-Planck description.

Two nondilute mechanisms are discussed in the electrokinetic literature, namely electrostatic correlations [33] and steric effects [33–36]. In particular, Khair and Squires [37] calculated the weak-field electrophoretic mobility of a spherical particle, including both steric effects and surface conduction, showing that steric effects can, in principle, reduce the effect of surface conduction.

The mean-field description of Poisson's equation breaks down because of electrostatic correlations, appearing when the characteristic distance between neighboring ions becomes comparable to the Bjerrum length

$$l^* = \frac{\mathcal{Z}^2 e^{*2}}{4\pi\epsilon^* k^* T^*}, \tag{7.1}$$

about 0.7 nm for monovalent aqueous solutions at room temperature. Steric effects, which modify the Nernst-Planck equations, are associated with the ionic diameter d^*, typically smaller than l^*, and are, hence, expected to appear at larger concentrations.

It is desirable to inspect the relative role of these mechanisms compared to surface conduction. Ion correlations appear when the characteristic zeta potential $\bar{\zeta}$ is large enough so that the typical separation associated with counterion concentration near the interface is comparable with the Bjerrum length. This concentration is estimated using the Boltzmann distribution of counterions; see (4.16). Since the (dimensional) value of the bulk salt is comparable to the ambient value c^*, the (much larger) counterion concentration near the interface is of order $c^* e^{\bar{\zeta}}$. We accordingly find that ion correlations appear at such (large enough) zeta potentials for which, roughly,

$$c^* e^{\bar{\zeta}} \sim \frac{1}{l^{*3}}. \tag{7.2}$$

The appearance of steric effects is characterized by a similar estimate, wherein l^* is replaced by d^*; this suggests that they are introduced at larger zeta potentials.

Unsurprisingly, both (7.2) and the criteria (5.2) for the appearance of surface conduction are expressed in terms of zeta-potential exponents. Substitution from Eq. (7.2) into (5.6) yields the critical Bikerman number $\mathrm{Bi}_{\mathrm{cr}} = \delta/(c^* l^{*3})^{1/2}$. Thus, when

$$O(1) \lesssim \mathrm{Bi} \lesssim \mathrm{Bi}_{\mathrm{cr}} \tag{7.3}$$

surface conduction plays a dominant role yet nondilute effects can be safely neglected (see Fig. 1). This is the regime in which our macroscale model for highly charged surfaces applies. It is useful to express the critical Bikerman number in terms of dimensional quantities. Thus, substitution of Eqs. (2.6) and (2.7) in conjunction with Eq. (2.1) yields

$$\mathrm{Bi}_{\mathrm{cr}} = \frac{1}{N_A}\left(\frac{\epsilon^* k^* T^*}{2\mathcal{Z}^2 e^{*2} l^{*3}}\right)^{1/2} \frac{1}{m^* a^*}. \tag{7.4}$$

This expression is written in terms of the ambient molar concentration $m^* = c^*/N_A$, in which N_A is Avogadro's number.

Expression (7.4) implies that the distinction between different systems essentially enters through the molar concentration m^*, the length scale a^*, and the ionic valency $\mathcal{Z}$. This suggests using (7.3) to identify those regions in the $(m^*, a^*, \mathcal{Z})$ parameter-space where surface conduction appears at large zeta potentials before nondilute effects become appreciable. Since surface conduction is introduced at $\mathrm{Bi} \sim O(1)$, these regions are identified by the asymptotic inequality $\mathrm{Bi}_{\mathrm{cr}} \gtrsim 1$. Using (7.1) and (7.4) for aqueous solutions at room temperature this inequality yields the restriction

$$m^* a^* \mathcal{Z}^4 \lesssim 6.80 \times 10^{-4}, \tag{7.5}$$

wherein m^* is measured in molars and a^* in microns. For given linear dimensions a^* of system, the concentration m^* must be lower than the value predicted by Eq. (7.5) for surface conduction to appear before nondilute effects.

Of course, for given a^*, the concentration must also be *large* enough so the Debye thickness is small compared with a^*, as stipulated. Considering, say, $\delta = 0.1$ as the upper bound for the thin-double-layer limit to practically apply, we obtain [see Eqs. (2.6) and (2.7)] the additional restriction

$$m^* a^{*2} \mathcal{Z}^2 \gtrsim 9.55 \times 10^{-6}. \tag{7.6}$$

Thus, for given a linear dimension a^*, the concentration m^* must be higher than the value predicted by Eq. (7.6) for the thin-double-layer limit to practically apply. Note, however, that for very large concentrations the Debye thickness is so small that the continuum description itself breaks down within the double layer. Roughly estimating the associated threshold value for the Debye thickness $1/\kappa^*$ as 10 Bjerram lengths, (2.7) and (7.1) then imply the additional constraint

$$m^* \mathcal{Z}^6 \lesssim 1.95 \times 10^{-3}. \tag{7.7}$$

For univalent systems, the decomposition of the (m^*, a^*) plane by the limiting curves corresponding to Eqs. (7.5)–(7.7) is depicted in Fig. 5. These curves delineate the region where (i) surface conduction precedes nondilute effects at large zeta potentials, (ii) the Debye layer is relatively thin, and (iii) the absolute Debye thickness is not too small. The corresponding regions for multivalent electrolytes are readily obtained from Eqs. (7.5)–(7.7).

VIII. RECAPITULATION

In this section we summarize the macroscale model derived in the preceding sections at the limit $\delta \to 0$. The differential equations governing electrokinetic transport within the

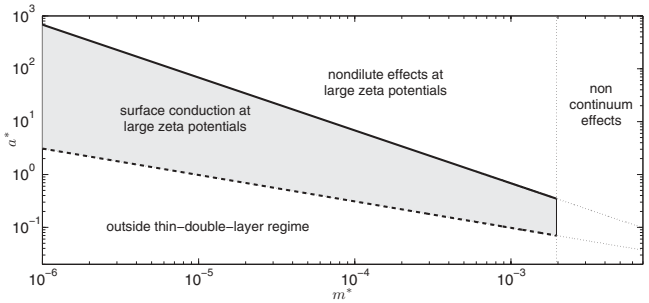

FIG. 5. Schematic decomposition of the (m^*,a^*) plane for univalent solutions, with m^* measured in molars and a^* in microns. The solid line depicts the limiting curve corresponding to Eq. (7.5): Above this line nondilute effects precede surface conduction at large zeta potentials. The dashed line depicts the limiting curve corresponding to Eq. (7.6): Below this line the thin-double-layer limit is inapplicable. The vertical thin line depicts the limiting curve corresponding to Eq. (7.7): To the right of this line the Debye layer is too thin for a continuum description to apply.

electroneutral bulk are as follows:

$$\nabla^2 c = \frac{\alpha^+ + \alpha^-}{2}\mathbf{u}\cdot\nabla c, \tag{8.1}$$

$$\nabla\cdot(c\nabla\varphi) = \frac{\alpha^+ - \alpha^-}{2}\mathbf{u}\cdot\nabla c, \tag{8.2}$$

$$\nabla\cdot\mathbf{u} = 0, \tag{8.3}$$

$$\nabla p = \nabla^2\mathbf{u} + \nabla^2\varphi\nabla\varphi. \tag{8.4}$$

The last equation represents the nill divergence of the sum of Newtonian

$$\mathsf{N} = -p\mathsf{I} + (\nabla\mathbf{u}) + (\nabla\mathbf{u})^\dagger \tag{8.5}$$

and Maxwell

$$\mathsf{M} = \nabla\varphi\nabla\varphi - \tfrac{1}{2}\nabla\varphi\cdot\nabla\varphi\,\mathsf{I} \tag{8.6}$$

stresses.

The effective boundary conditions specified on the asymptotic boundary s depend on the surface-charge scaling.

A. Moderately charged surfaces

In this classical limit of the boundary conditions consist of the homogenous Neumann conditions

$$\frac{\partial\varphi}{\partial n} = 0, \quad \frac{\partial c}{\partial n} = 0, \tag{8.7}$$

together with the Dukhin-Derjaguin slip condition

$$\mathbf{u} = \zeta\nabla_s\varphi + 2\ln\left(1 - \tanh^2\frac{\zeta}{4}\right)\nabla_s\ln c, \tag{8.8}$$

obtained from Eqs. (4.32)–(4.33). In this condition the operator

$$\nabla_s = (\mathsf{I} - \hat{\mathbf{n}}\hat{\mathbf{n}})\cdot\nabla \tag{8.9}$$

is the surface gradient; it may, however, be replaced by ∇ in view of Eq. (8.7). The zeta potential ζ appearing in Eq. (8.8) is related to the $O(1)$ charge density σ through the relation

$$\sigma = 2\sqrt{c}\sinh\frac{\zeta}{2}. \tag{8.10}$$

B. Highly charged surfaces

For highly charged surfaces, where $\sigma \sim O(\delta^{-1})$, the effective boundary conditions are modified. Consider, first, the case $\sigma > 0$. Conditions (8.7) are replaced by the inhomogeneous conditions

$$\frac{\partial c}{\partial n} + c\frac{\partial\varphi}{\partial n} = 0, \tag{8.11a}$$

$$\frac{\partial c}{\partial n} = \mathrm{Bi}(1 + 2\alpha^-)\nabla_s^2(\varphi - \ln c), \tag{8.11b}$$

wherein the Bikerman number is defined as $\mathrm{Bi} = \delta\sigma$. The dimensionless group

$$\mathrm{Du} = \mathrm{Bi}(1 + 2\alpha^-) \tag{8.12}$$

superficially resembles the Dukhin number employed in the literature; note, however, that it is not defined here in terms of a "zeta potential." In the prevailing weak-field description, where ionic advection is negligible outside the double layer, α^- appears in the macroscale model only through this combination; it is then useful to employ Du instead of Bi throughout. In the present macroscale description, which is not limited to weak fields, advection appears also in the leading-order bulk transport [see (8.1) and (8.2)], and it is advantageous to use the more fundamental Bikerman number.

The slip condition (8.8) is also modified. Use of Eq. (4.32) and (6.52) yields, in an invariant notation,

$$\mathbf{u} = 4\ln 2\nabla_s\ln c + \zeta\nabla_s(\varphi - \ln c) \tag{8.13}$$

wherein

$$\zeta = 2\ln\sigma - \ln c. \tag{8.14}$$

Here, the surface-gradient operator ∇_s appearing in Eq. (8.13) cannot be replaced by ∇. Note that the second term in Eq. (8.13) is logarithmically large in δ; its appearance in our leading order description is consistent with our asymptotic methodology. A uniform approximation valid for both small and moderate Bikerman numbers is simply provided by the moderate-charge model, when (8.7) are replaced by Eq. (8.11).

For $\sigma < 0$ it is readily verified that (8.11)–(8.14) remain valid provided we replace α^- with α^+ in Eq. (8.12), φ with $-\varphi$ in Eqs. (8.11) and (8.13), ζ with $-\zeta$ in Eq. (8.13). In Eq. (8.14), $2\ln\sigma$ and $\ln c$ are respectively replaced with $-2\ln(-\sigma)$ and $-\ln c$. The Bikerman number is now defined as $\mathrm{Bi} = -\delta\sigma$ [cf. (5.3)].

Note that a weak-field linearization of the preceding equations furnishes the classical model of O'Brien [8].

IX. ELECTROPHORESIS OF A SPHERICAL PARTICLE

Consider now the thin-double-layer limit of the electrophoresis problem defined at the end of Sec. II. We employ spherical polar coordinates (r,θ) with $r = 0$ coinciding with the particle center and $\theta = 0$ in the applied field direction. Thus, the far-field conditions read

$$c \to 1, \quad \varphi \sim -\beta r\cos\theta, \quad \mathbf{u} \to -\mathscr{U}\hat{\boldsymbol{\imath}}. \tag{9.1}$$

In applying the force-free condition we note that by symmetry there can be no force in a direction perpendicular to $\hat{\boldsymbol{\imath}}$ and,

hence, replace (2.20) with the scalar constraint

$$\oint dA\, \hat{\mathbf{n}} \cdot (\mathsf{N} + \mathsf{M}) \cdot \hat{\boldsymbol{\imath}} = 0, \tag{9.2}$$

wherein the integration domain may be chosen as any closed surface within the bulk that encloses the particle.

A. Moderately charged particle

For a moderately charged particle it is readily verified that the solution of equations (8.1) and (8.7) is the uniform concentration

$$c \equiv 1. \tag{9.3}$$

Thus, (8.2)–(8.4) degenerate to a linear system consisting of Laplace's equation

$$\nabla^2 \varphi = 0 \tag{9.4}$$

and the homogeneous Stokes equations

$$\boldsymbol{\nabla} p = \nabla^2 \mathbf{u} \tag{9.5}$$

while the slip condition (8.8) degenerates to the linear Helmholtz–Smoluchowski form,

$$\mathbf{u} = \zeta \boldsymbol{\nabla} \varphi \quad \text{on} \quad s. \tag{9.6}$$

In view of Eq. (9.3), the zeta potential distribution [see (8.10)] becomes a uniform one, defined by $\sigma = 2\sinh(\zeta/2)$.

It is well known from the properties of the harmonic problem defined by Eqs. (8.7), (9.1), and (9.5) that the electric field decays at most like r^{-3} to its uniform value at infinity [38]. For this dipole decay, the Maxwell stresses result in a zero resultant force [39,40]. The electrokinetic problem has therefore become linear. As observed by Morrison [41], the solution to this problem is provided by the potential flow

$$\mathbf{u} = \zeta \boldsymbol{\nabla} \varphi \tag{9.7}$$

with zero pressure: (i) As with any irrotational flow, it identically satisfies the Stokes equation (8.4), (ii) because φ is harmonic it clearly satisfies the continuity equation (8.3), (iii) it evidently satisfies the slip condition Eq. (9.6), and (iv) by extending the integration surface in Eq. (9.2) to infinity, where the Newtonian stress is $O(r^{-4})$, it is readily verified that the force-free constraint is satisfied.

Solution Eq. (9.7) together with Eq. (9.1) therefore provides the Smoluchowski formula

$$\mathscr{U} = \beta\zeta. \tag{9.8}$$

While linear in β, the present analysis clearly reveals that it is *not* limited to small β and should not be interpreted as a weak-field approximation—a common misconception in the literature. (As a matter of fact, a moderate-surface-charge analysis for large β values, scaling as δ^{-1}, reveals that Smoluchowski's formula approximately holds even then; see Ref. [42].)

While the present electrophoretic problem has been formulated for a spherical particle, its results equally hold for any particle shape [41]. In that general case, one only needs to prove that the particle is also torque free, which again readily follows from the decay properties of the electric field and presumed potential flow Eq. (9.7).

B. Highly charged particle

For a highly charged surface the uniform concentration (9.3) is incompatible with Eq. (8.11); the electrophoretic problem is inherently nonlinear, whereby particle motion is additionally affected by diffuso-osmotic slip and Maxwell stresses, the latter playing a role both locally, through Coulomb body forces, and globally, contributing to the resultant force on the particle. In general, these mechanisms are of comparable magnitude to electro-osmotic slip, which is the only mechanism acting under conditions of uniform concentration. In contrast to the case of moderately charged particle, an analytic solution for arbitrary β values is unavailable. (Clearly, one should not expect a linear variation with β.)

A solution can be obtained for weakly applied fields,

$$\beta \ll 1. \tag{9.9}$$

In this limit, we employ the rescaling

$$c = 1 + \beta \grave{c}, \quad \varphi = \beta \grave{\varphi}, \quad \mathbf{u} = \beta \grave{\mathbf{u}}, \quad p = \beta \grave{p} \tag{9.10}$$

and

$$\mathscr{U} = \beta \grave{\mathscr{U}}. \tag{9.11}$$

At leading order (8.1)–(8.4) yield the linearized equations

$$\nabla^2 \grave{c} = 0, \quad \nabla^2 \grave{\varphi} = 0, \quad \boldsymbol{\nabla} \cdot \grave{\mathbf{u}} = 0, \quad \boldsymbol{\nabla} \grave{p} = \nabla^2 \grave{\mathbf{u}}; \tag{9.12}$$

conditions (8.11) become [see (8.12)]

$$\frac{\partial \grave{c}}{\partial n} + \frac{\partial \grave{\varphi}}{\partial n} = 0, \quad \frac{\partial \grave{c}}{\partial n} = \mathrm{Du} \nabla_s^2 (\grave{\varphi} - \grave{c}), \tag{9.13}$$

and the slip condition (8.13) yields

$$\grave{\mathbf{u}} = 4 \ln 2 \boldsymbol{\nabla}_s \grave{c} + \bar{\zeta} \boldsymbol{\nabla}_s (\grave{\varphi} - \grave{c}), \tag{9.14}$$

where $\bar{\zeta} = 2\ln\sigma$ is the uniform zeta potential of the unperturbed solution. In terms of the scaled variables, the far-field conditions (9.1) read

$$\grave{c} \to 0, \quad \grave{\varphi} \sim -r\cos\theta, \quad \grave{\mathbf{u}} \to -\grave{\mathscr{U}} \hat{\boldsymbol{\imath}}, \tag{9.15}$$

while the Maxwell stresses disappear from the force-free constraint (9.2):

$$\oint dA\, \hat{\mathbf{n}} \cdot \{-\grave{p}\mathsf{I} + \boldsymbol{\nabla}\grave{\mathbf{u}} + (\boldsymbol{\nabla}\grave{\mathbf{u}})^{\dagger}\} \cdot \hat{\boldsymbol{\imath}} = 0. \tag{9.16}$$

The preceding linear problem is semicoupled. The salt concentration and electric potential are independent of the flow and are given by

$$\grave{c} = -\frac{3\mathrm{Du}}{1+2\mathrm{Du}} \frac{\cos\theta}{2r^2}, \quad \grave{\varphi} = -\left\{ r + \frac{1}{2r^2} \frac{1-\mathrm{Du}}{1+2\mathrm{Du}} \right\} \cos\theta. \tag{9.17}$$

The slip velocity (9.14) is, then,

$$\grave{\mathbf{u}} = \frac{3}{2} \frac{\bar{\zeta} + \mathrm{Du}\ln 16}{1+2\mathrm{Du}} \hat{\mathbf{e}}_\theta \sin\theta. \tag{9.18}$$

The linearity of the flow problem allows us to decompose it into two parts, both satisfying the continuity and Stokes equations. The first part satisfies the slip condition (9.18) together with zero velocity at infinity, while the second part satisfies a no-slip condition on s together with the uniform stream condition (9.15). Using a variant of the reciprocal theorem [43], the hydrodynamic force on the particle (in the $\hat{\boldsymbol{\imath}}$

direction) associated with the first part given by

$$-3\pi \int_0^{\pi} \hat{\mathbf{i}} \cdot \grave{\mathbf{u}} \sin\theta \, d\theta; \tag{9.19}$$

the force associated with the second problem is simply the Stokes drag, $-6\pi \grave{\mathscr{U}}$. Thus, the velocity $\grave{\mathscr{U}}$ is readily obtained from Eq. (9.16) without the need to solve the flow problem. Substitution of Eq. (9.18) into (9.19) furnishes the velocity

$$\grave{\mathscr{U}} = \frac{\bar{\zeta} + \mathrm{Du} \ln 16}{1 + 2\mathrm{Du}}, \tag{9.20}$$

in agreement with O'Brien and Hunter [7]. In the present context, Morrison's generalization does not hold, and (9.20) strictly applies to a spherical shape.

The remarkable ease by which Dukhin's mobility (9.20) is obtained is to be contrasted with the mathematically involved classical derivations of this result (cf. Ref. [7]). The difference in the derivations has to do with with the order of the limit processes involved. In the present scheme we first consider the thin-double-layer limit and only then the weak-field approximation; formally, this is the proper sequence since the first (singular) limit is essentially associated with a geometric decomposition of the fluid domain while the second limit is a regular expansion in a small parameter. The reverse order used in the existing literature entails first a weak-field linearization; the breakdown of this approximation outside the double layer, where the leading-order equilibrium variables decay exponentially fast, becomes only more pronounced when the double layer becomes narrow.

X. CONCLUDING REMARKS

We have developed a macroscale model for electrokinetic flows at the thin-double-layer limit, addressing both moderately charged and highly charged solid surfaces. This model comprises approximate differential equations, describing transport in the essentially electroneutral bulk surrounding the double layer, as well as effective boundary conditions representing the double-layer physics. Not being restricted to the weak-field regime, it may be useful for analyzing the rich spectrum of nonlinear phenomena observed in practice [18], which clearly reside outside the scope of classical weak-field theories. Since the scale disparity associated with the thin-double-layer limit has been effectively removed, our scheme is natural for use in numerical simulations.

A novel feature in our analysis of highly charged surfaces is the explicit decomposition of the diffuse part of the double layer into an "outer" Debye layer and an "inner" Dukhin layer, the latter characterized by an asymptotically large counterion concentration. The high-charge limit is accordingly analyzed via an appropriate double limit, of asymptotically small Debye thickness and fixed Bikerman number, where separate asymptotic expansions are introduced in the two layers. This systematic approach is superior to the intuitive procedures prevailing in weak-field investigations of this limit.

The set of bulk differential equations is identical in both the moderate- and high-charge classes of problems. Although the electrolyte is approximately electroneutral, its concentration is generally nonuniform, governed by an advective-diffusive equation governing this variable. Charge conservation provides an elliptic differential equation governing the electric potential, wherein the salt concentration constitutes an effective conductivity; in the case of a uniform salt distribution, this equation degenerates to Laplace's equation. Despite leading-order electroneutrality, Coulomb body forces appear in the leading-order momentum balance; these forces are relegated to higher orders when the salt concentration is uniform.

The difference between the moderate- and high-charge classes appears in the effective boundary conditions: thus, the homogenous conditions in the moderate-charge limit are replaced by comparable inhomogeneous conditions, accounting for the emergence of transverse counterion flux at leading order. These conditions [see (8.11)] are expressed in terms of the nonlinear chemical potentials of both ionic species. This difference gives rise to a fundamental distinction between the two classes. For moderate surface charge, salt polarization is introduced only through externally imposed salt-concentration gradients; at the high-charge limit, on the other hand, it is inevitable at any out-of-equilibrium scenario. The latter limit is, hence, intrinsically nonlinear.

With an ingrained inhomogeneous salt distribution, the zeta potential is nonuniform even for uniformly charged solid surfaces. The "particle zeta-potential" concept therefore loses its usual interpretation. In defining an appropriate parameter whose values reflects the specific limit at hand, we need to identify a global quantity which scales essentially as $\exp(\zeta/2)$ but does not vary along the surface; this quantity is provided by the (dimensionless) surface charge density. The resulting dimensionless group, denoted here the Bikerman number Bi, effectively entails the zeta-potential value corresponding to equilibrium, where the bulk concentration is uniform. The transition from asymptotically small Bi at moderate zeta potentials to $\mathrm{Bi} \sim O(1)$ at logarithmically large zeta potentials reflects the appearance of surface conduction at the dominant macroscale transport.

This need for a careful definition of a dimensionless number was apparently overlooked in the literature, perhaps because of the prevailing focus on weak-field linearization, where the zeta-potential nonuniformity does not affect the leading-order mobility calculations. Outside of that linear regime, however, this nonuniformity cannot be neglected; the zeta-potential polarization therefore plays a major role for $\mathrm{Bi} \sim O(1)$, where concentration variations are inevitable.

The inherent spatial variation of the zeta potential should not be confused with zeta-potential variations associated with the electric displacement induced within the dielectric solid (colloquially associated with "induced-charge" mechanisms; see Ref. [44]). Unless the ratio of solid-to-electrolyte permittivities is $O(1/\delta)$ large [45,46], such variations enter the leading-order description only in the presence of geometric singularities, e.g., sharp corners [47,48]. In our analysis, where we implicitly assume that this ratio is moderate, such variations would only affect higher-order corrections. (In reality, this ratio is actually quite small; see Ref. [28]).

To illustrate our macroscale model we apply it to the prototypic problem of spherical particle electrophoresis, where the differences between the moderate-charge and high-charge limits are significant. At the moderate-charge limit the bulk concentration turns out uniform, whereby the originally nonlinear macroscale problem degenerates to a linear one. The

particle accordingly moves with the Smoluchowski velocity at all field strengths. At the high-charge limit the problem is inherently nonlinear; solving it in the weak-field limit yields the mobility expression of O'Brien and Hunter [7].

The derived macroscale model is reminiscent of that appropriate to phoretic motion of ion-selective particles [49], where the particle boundary allows for ion-exchange of one of the ionic species. Both problems share an inherent asymmetry, where one of the two ionic transverse fluxes within the Debye layer is nonzero; in the present problem, it is the flux associated with the counterions, while in the problem of ion-selective surface it is the one associated with the "reactive" ionic species. In both scenarios this flux inevitably results in bulk concentration gradients.

In deriving our model, we have utilized a rather generic problem formulation, not limited to any specific problem or geometry. While illustrated here only for the prototypic problem of sphere electrophoresis, it can be applied in other situations as well. For brevity, however, we did not consider the most general scenario. Thus, for instance, we have assumed a steady-state transport. While this assumption is consistent with a significant number of applications (electro-osmosis in a channel, electrophoresis of axisymmetric particles, etc.) it breaks down when considering the motion of several particles, where unsteadiness is introduced through the motion of the boundaries. Fortunately, our scheme is easily generalized to unsteady processes; see Ref. [50].

Another limiting assumption is that of a uniform-surface charge distribution on the solid boundary. This assumption was deliberately introduced to emphasize the inherent nonuniformity in the zeta potential distribution; as a matter of fact, it is readily verified that the macroscale model for the moderate-charge limit remains valid even for a nonuniform distribution of σ (still presumably prescribed). The generalization of the high-charge limit to such nonuniform distributions is a rather formal matter of proper definitions, where the Bikerman number is defined through some characteristic value of σ. Of course, one could envision a more fundamental model where the physicochemical surface-charge regulation process itself is accounted for; see, e.g., Ref. [51].

In the high-charge limit, the derived macroscale model may stimulate numerous research directions, of which we survey just a few. The weakly nonlinear analysis of weak-field electrophoresis ($\beta \ll 1$), constituting a natural extension of the present illustration, will constitute the subject of a future publication. The related numerical simulations for moderate fields [$\beta \sim O(1)$] and asymptotic analysis of the strong-field limit ($\beta \gg 1$) are currently in process. Similar nonlinear extensions are also desirable in the modeling of particle diffuso-phoresis. This problem was analyzed by Prieve *et al*. [52] for moderate surface-charge density and by Pawar *et al*. [13] for high charge density; both analyses are based on the assumption of a weakly applied salt gradient. The situation here is more complicated than that in the electrophoretic problem, since the linear solution obtained for moderate surface charge density only holds for weak fields. Moreover, when going beyond linear response in diffuse-phoretic problems, the imposed-salt-gradient condition, which constitutes a local approximation in the particle vicinity, must be replaced by a realistic condition representing the imposed salt nonuniformity; in a true nonlinear scheme, an artificial salt-gradient condition inevitably leads to the nonphysical prediction of negative concentrations. These issues are well known in the context of particle thermophoresis by imposed temperature differences [53].

Other directions may involve nonspherical particles. In the moderate-charge limit it is common knowledge [41] that any particle would translate with Smoluchowski's electrophoretic velocity (and would not rotate); this is true regardless of its size, shape, or orientation relative to the uniformly applied field. This remarkable property is invalid in the high-charge limit; indeed, the weak-field analysis of O'Brien and Hunter [7] leads to a size-dependent electrophoretic mobility [see Eq. (9.20)]. A comparable weak-field analysis for a spheroidal particle was carried out by O'Brien and Ward [54]; while their linearized calculation does not predict particle rotation, they claim it should appear at $O(\beta^2)$. Our model provides the framework for carrying out the requisite weakly nonlinear analysis for calculating this rotation effect. Finally, since Sellier's extension [55] of Morrison's single-particle analysis to a cluster of particles does not hold in the high-charge limit, it may be of interest to apply our model for analyzing the effect of surface conduction on electrokinetic particle interactions.

ACKNOWLEDGMENTS

We thank Aditya Khair for useful discussions. This work was supported by the Israel Science Foundation (Grant No. 114/09).

[1] M. Smoluchowski, Bull. Inter. Acad. Sci. Cracovie **184**, 199 (1903).
[2] P. H. Wiersema, A. L. Loeb, and J. T. G. Overbeek, J. Colloid Interface Sci. **22**, 78 (1966).
[3] R. W. O'Brien and L. R. White, J. Chem. Soc., Faraday Trans. **74**, 1607 (1978).
[4] S. S. Dukhin, in *Twentieth Intl Cong. on Pure and Applied Chemistry*, Vol. A 72 (Moscow, 1965), p. 68.
[5] S. S. Dukhin and V. Shilov, Colloid J. USSR **31**, 564 (1969).
[6] J. Bikerman, Trans. Faraday Soc. **35**, 154 (1940).
[7] R. W. O'Brien and R. J. Hunter, Can. J. Chem. **59**, 1878 (1981).
[8] R. W. O'Brien, J. Colloid Interface Sci. **92**, 204 (1983).
[9] J. D. Sherwood, J. Fluid Mech. **101**, 609 (1980).
[10] E. J. Hinch and J. D. Sherwood, J. Fluid Mech. **132**, 337 (1983).
[11] W. Chew, J. Chem. Phys. **80**, 4541 (1984).
[12] E. J. Hinch, J. D. Sherwood, W. C. Chew, and P. N. Sen, J. Chem. Soc., Faraday Trans. 2 **80**, 535 (1984).
[13] Y. Pawar, Y. Solomentsev, and J. Anderson, J. Colloid Interface Sci. **155**, 488 (1993).
[14] A. Khair and T. Squires, Phys. Fluids **20**, 087102 (2008).
[15] E. Yariv, J. Fluid Mech. **521**, 181 (2004).

[16] A. Khair and T. Squires, J. Fluid Mech. **615**, 323 (2008).
[17] A. Khair and T. Squires, Phys. Fluids **21**, 042001 (2009).
[18] H.-C. Chang and L. Y. Yeo, *Electrokinetically Driven Microfluidics and Nanofluidics* (Cambridge University Press, Cambridge, UK, 2010).
[19] K. T. Chu and M. Z. Bazant, Phys. Rev. E **74**, 011501 (2006).
[20] J. L. Anderson, Annu. Rev. Fluid Mech. **30**, 139 (1989).
[21] H. J. Keh and J. L. Anderson, J. Fluid Mech. **153**, 417 (1985).
[22] S. Ghosal, J. Fluid Mech. **459**, 103 (2002).
[23] E. Yariv and H. Brenner, J. Fluid Mech. **484**, 85 (2003).
[24] E. Yariv, J. Fluid Mech. **613**, 85 (2008).
[25] A. Sellier, C. R. Acad. Sci., Ser. IIb: Mec. **329**, 47 (2001).
[26] J. S. Newman, *Electrochemical Systems* (Prentice-Hall, Englewood Cliffs, NJ, 1973).
[27] M. Van Dyke, *Perturbation Methods in Fluid Mechanics* (Academic Press, New York, 1964).
[28] D. A. Saville, Annu. Rev. Fluid Mech. **9**, 321 (1977).
[29] R. G. Cox, J. Fluid Mech. **338**, 1 (1997).
[30] I. Rubinstein and B. Zaltzman, Math. Models Methods Appl. Sci. **11**, 263 (2001).
[31] E. J. Hinch, *Perturbation Methods* (Cambridge University Press, Cambridge, 1991).
[32] C. Bender and S. Orszag, *Advanced Mathematical Methods for Scientists and Engineers* (McGraw-Hill, New York, 1978).
[33] M. Z. Bazant, M. S. Kilic, B. D. Storey, and A. Ajdari, Adv. Colloid Interface Sci. **152**, 48 (2009).
[34] P. M. Biesheuvel and M. van Soestbergen, J. Colloid Interface Sci. **316**, 490 (2007).
[35] M. S. Kilic, M. Z. Bazant, and A. Ajdari, Phys. Rev. E **75**, 021502 (2007).
[36] M. S. Kilic, M. Z. Bazant, and A. Ajdari, Phys. Rev. E **75**, 021503 (2007).
[37] A. Khair and T. Squires, J. Fluid Mech. **640**, 343 (2009).
[38] G. K. Batchelor, *An Introduction to Fluid Dynamics* (Cambridge University Press, Cambridge, 1967).
[39] N. J. Rivette and J. C. Baygents, Chem. Eng. Sci. **51**, 5205 (1996).
[40] E. Yariv, Phys. Fluids **18**, 031702 (2006).
[41] F. A. Morrison, J. Colloid Interface Sci. **34**, 210 (1970).
[42] O. Schnitzer and E. Yariv, J. Fluid Mech. **701**, 333 (2012).
[43] H. Brenner, Chem. Eng. Sci. **19**, 703 (1964).
[44] T. M. Squires and M. Z. Bazant, J. Fluid Mech. **509**, 217 (2004).
[45] G. Yossifon, I. Frankel, and T. Miloh, Phys. Fluids **19**, 068105 (2007).
[46] E. Yariv and A. Davis, Phys. Fluids **22**, 052006 (2010).
[47] S. K. Thamida and H.-C. Chang, Phys. Fluids **14**, 4315 (2002).
[48] G. Yossifon, I. Frankel, and T. Miloh, Phys. Fluids **18**, 117108 (2006).
[49] E. Yariv, J. Fluid Mech. **655**, 105 (2010).
[50] E. Yariv, O. Schnitzer, and I. Frankel, J. Fluid Mech. **685**, 306 (2011).
[51] M. B. Andersen, J. Frey, S. Pennathur, and H. Bruus, J. Colloid Interface Sci. **353**, 301 (2011).
[52] D. C. Prieve, J. P. Ebel, J. L. Anderson, and M. E. Lowell, J. Fluid Mech. **148**, 247 (1984).
[53] E. Yariv, SIAM J. Appl. Math. **69**, 453 (2008).
[54] R. O'Brien and D. Ward, J. Colloid Interface Sci. **121**, 402 (1988).
[55] A. Sellier, C. R. Acad. Sci., Ser. IIb: Mec. **327**, 443 (1999).